Supporting Information

Parametric analysis of a gasification-based cookstove as a function of biomass density, gasification behavior, airflow ratio, and design

Jonatan Gutiérrez [1,2], Edwin Lenin Chica [2], Juan F. Pérez [1,*]

[1] Grupo de Manejo Eficiente de la Energía – GIMEL, Departamento de Ingeniería Mecánica, Facultad de Ingeniería, Universidad de Antioquia, Calle 67, No. 53-108 Medellín (Colombia)

[2] Grupo de Energía Alternativa – GEA, Departamento de Ingeniería Mecánica, Facultad de Ingeniería, Universidad de Antioquia, Calle 67, No. 53-108 Medellín (Colombia)

*Corresponding : Juan F. Pérez, Phone: (+57 604) 2198552; e-mail: juanpb@udea.edu.co

S1. Modified WBT protocol

Table S1. Procedure for executing the modified WBT 4.2.3 protocol.

Stage: CS.S1	
Procedure	Measured variables
1. Start of CS, ignition of the cookstove.	$m_{w,iS1}$: initial water mass S1 [g] $m_{bms,iS1}$: initial biomass mass S1 [g] T_{wiS1}: initial water temperature S1 [°C]
2. Wait until the water reaches the boiling temperature, remove the pot from the cookstove and record the values of the variables.	$m_{w,fS1}$: final water mass S1 [g] $m_{bms,iS1}$: final biomass mass S1 [g] T_{wfS1}: final water temperature S1 [°C] t_{S1}: time spent during the S1 stage [s]
Stage: CS.S2	
3. Put the pot back on the cookstove with the water boiled in cold start - stage 1.	$m_{w,iS2}$: initial water mass S2 [g] $m_{bms,iS2}$: initial biomass mass S2 [g] T_{wiS2}: initial water temperature S2 [°C]
4. Keep the water at boiling temperature until a final biomass amount of ~200 g is reached in the bed. Remove the pot and record the values of the variables.	$m_{w,fS2}$: final water mass S2 [g] $m_{bms,fS2}$: final biomass mass S2 [g] T_{wfS2}: final water temperature S2 [°C] t_{S2}: time spent during the S2 stage [s]
5. Leave the cookstove running until the flame is completely blue, which indicates that only biochar remains in the bed.[18]	$m_{biochar}$: biochar mass [g]

S2. Calculation model of WBT parameters

Table S2 shows how with the measured data in each start and their respective stages, the process variables indicated in Eqs. (S1)-(S11) were calculated, in order to finally determine the TLUD cookstove performance by efficiency (%), specific energy consumption (kJ/L), and specific energy consumption per unit time (kJ/L-min) by using Eq. (S12), (S13), and (S14), respectively. The environmental parameters, such as specific emissions of CO -EF_{CO}- (g/MJ_d) and specific emissions of total suspended particulate matter -EF_{TSPM}-(mg/MJ_d), were calculated by Eq. (S15) and Eq. (S16), respectively. Both specific emissions were calculated based on the energy delivered to the water (MJ_d).[86]

Table S2. Parameters calculation model of the WBT 4.2.3 protocol [85].

Parameter	Model	Eq.
Mass of boiling water (m_{wb}, g)	$m_{w,b} = m_{w,i} - m_{ce}$ where: $m_{w,i}$ (g): initial water mass = water mass (g) + mass of the pot (g). m_{ce}: the mass of the pot (g).	(S1)
Mass of evaporated water ($m_{w,e}$, g)	$m_{w,e} = m_{w,i} - m_{w,f}$ where:	(S2)

	$m_{w,f}$ (g): final water mass=water mass (g)+mass of the pot (g).	
Energy of boiled water ($E_{w,b}$, J)	$$E_{w,b} = m_{w,b} \cdot C_{p,water} \cdot (T_{w,f} - T_{w,i})$$ where: $C_{p,water}$: the specific heat of water (4.18 kJ/kg/K). $T_{w,f}$: final water temperature (°C). $T_{w,i}$: initial water temperature (°C).	(S3)
Energy evaporated water ($E_{w,e}$, J)	$$E_{w,e} = m_{w,e} \cdot h_{fg}$$ where: h_{fg}: latent heat of water evaporation (2260 kJ/kg).	(S4)
Total energy supplied to the water ($E_{w,t}$, J)	$$E_{w,t} = E_{w,b} + E_{w,e}$$	(S5)
Mass of biomass consumed ($m_{bms,c}$, g)	$$m_{bms,c} = m_{bms,i} - m_{bms,f}$$ where: $m_{bms,i}$: initial biomass mass (g). $m_{bms,f}$: final biomass mass (g).	(S6)
Dry mass of biomass consumed ($m_{bms,c,d}$, g)	$$m_{bms,c,d} = m_{bms,c} \cdot (1 - MC)$$ where: MC: moisture content of biomass (g/g).	(S7)
Biochar mass yield ($Y_{biochar}$, %)	$$Y_{biochar} = \frac{m_{biochar}}{m_{bms,i}}$$	(S8)
Biochar mass (m_c, g)	$$m_c = Y_{biochar} * m_{bms,c}$$	(S9)
Energy to evaporate moisture from biomass ($E_{e,w,bms}$, J)	$$E_{e,w,bms} = m_{bms,c} \cdot MC \cdot (C_{p,water} \cdot (T_{d,bms} - T_i) + h_{fg})$$ where: $T_{d,bms}$: Biomass drying temperature (103 °C).	(S10)
Energy supplied by biomass to boil-evaporate water ($E_{s,bms}$, J)	$$E_{s,bms} = m_{bms,c,d} \cdot LHV_{bms} - m_c \cdot LHV_{biochar} - E_{e,w,bms}$$ where: LHV_{bms}: lower heating value of biomass (kJ/kg). LHV_{char}: lower heating value of biochar (28800 kJ/kg and 27920 kJ/kg for pellets biochar and chips biochar, respectively)[77].	(S11)
Energy efficiency of the cookstove (η, %)	$$\eta = \frac{E_{w,t}}{E_{s,bms}} \cdot 100$$	(S12)
Specific energy consumption (SFEC, kJ/L)	$$SFEC = \frac{m_{bms,c} \cdot \rho_w}{m_{w,b}} \cdot \frac{LHV_{bms}}{1000}$$ where: ρ_w = water density (1000 kg/m^3).	(S13)
Specific energy consumption per unit time (SFCT, kJ/L-min)	$$SFCT = \frac{SFEC \cdot 60}{t_{test}}$$	(S14)
CO specific emissions (EF_{CO}, g/MJ$_d$)[86]	$$EF_{CO} = \frac{m_{CO}}{E_{w,t\,S1} + E_{w,t\,S2}}$$ where: m_{CO} = mass of CO, determined from the measured concentrations with the flue gas analyzer and by using mass balances. $E_{w,t\,sj}$= total energy supplied to the water in each stage (J). Eq. (S5).	(S15)

TSPM specific emissions (EF_{TSPM}, mg/MJ_d)[86]	$$EF_{TSPM} = \frac{m_{TSPM}}{E_{w,t\,S1} + E_{w,t\,S2}} \cdot \frac{\dot{V}_{duct}}{\dot{V}_{vacuum\ pump}}$$ where: m_{TSPM} = mass of TSPM, determined by gravimetry. $\dot{V}_{duct}$ = total volume of gases flowing through the dilution line during the test (m^3/s) $\dot{V}_{vacuum\ pump}$ = volumetric flow rate of the vacuum pump (m^3/s)	(S16)

S3. Statistical design of the experiments

S3.1. Gasification-based biomass cookstove (CV_1)

The TLUD cookstove characterization (CV_1) was carried out in two sections. In the first section, the factors and their levels were the biomass bulk density (2 levels, 560 kg/m^3 -pellets-, and 151 kg/m^3 -chips-), the combustion-air/gasification-air ratio (3 levels, 2.8, 3.0, and 3.2), and the combustion chamber design (2 levels, combustion chamber 1 and 2). These factors were evaluated following the modified WBT 4.2.3 protocol during stage 1 (until water reaches boiling temperature),[48,52,58] both in cold start and hot start (cold start - stage 1 and hot start - stage 1). The combination of the levels for each factor resulted in 12 experimental tests. Each experiment was carried out twice, leading to 24 tests. The start (cold and hot) was included as a factor in the analysis of the results. Therefore, a design of mixed levels 3×2^3 was adopted, whose model is presented in Eq. (S17).[89] The aim is to study the significance of the factors on the cookstove response variables: efficiency (%), specific energy consumption (kJ/L), specific energy consumption per unit time (kJ/L-min), and specific emissions of CO (g/MJ_d).

$$Y_{ijklm} = \mu + \tau_i + \beta_j + \gamma_k + \rho_l + (\tau\beta)_{ij} + (\tau\gamma)_{ik} + (\tau\rho)_{il} + (\beta\gamma)_{jk} + (\beta\rho)_{jl} + (\gamma\rho)_{kl} + (\tau\beta\gamma)_{ijk} + (\tau\gamma\rho)_{ikl} + (\beta\gamma\rho)_{jkl} + (\tau\beta\gamma\rho)_{ijkl} + \varepsilon_{ijklm} \quad \text{(S17)}$$

where μ is the global measure; τ_i is the effect of factor A; β_j is the effect of factor B; γ_k corresponds to the effect of factor C; ρ_l is the effect of factor D; $(\tau\beta)_{ij}$, $(\tau\gamma)_{ik}$, $(\tau\rho)_{ik}$, $(\beta\gamma)_{jk}$, $(\beta\rho)_{ik}$, and $(\gamma\rho)_{ik}$ are the interactions between each pair of factors; $(\tau\beta\gamma)_{ijk}$, $(\tau\gamma\rho)_{ikl}$, and $(\beta\gamma\rho)_{jkl}$ correspond to the interactions among three factors; $(\tau\beta\gamma\rho)_{ijkl}$ is the interaction among the four factors, and ε_{ijklm} is the error.[89]

The specific emissions of total suspended particle matter was measured for the pellets (560 kg/m^3 bulk density) because this biomass type reached a better energy performance and lower pollutant emissions, according to the first stage of the study described above. A full factorial design with three factors was adapted for the specific emissions of total suspended particle matter, whose model is presented in Eq. (S18),[89] and the modified WBT 4.2.3 protocol was executed completely, whereby, in each experimental test the stages cold start and hot start (cold start - stage 1, cold start - stage 2, hot start - stage 1, and hot start - stage 2) were executed. The assessed factors and their levels were the combustion-air/gasification-air ratio (3 levels, 2.8, 3.0, and 3.2), and the combustion

chamber design (2 levels, combustion chamber 1 and 2). Each experiment was carried out twice, resulting in 12 tests. The starts type of the WBT protocol (cold start and hot start) were included in the analysis as a factor. Finally, ANOVA was carried out in order to evaluate the effect of experimental factors on FE_{TSPM} (mg/MJ_d).

$$Y_{ijkl} = \mu + \tau_i + \beta_j + \gamma_k + (\tau\beta)_{ij} + (\tau\gamma)_{ik} + (\beta\gamma)_{jk} + (\tau\beta\gamma)_{ijk} + \varepsilon_{ijkl} \quad \text{(S18)}$$

where μ is the global measure; τ_i is the effect of factor A; β_j is the effect of factor B; γ_k corresponds to the effect of factor C; $(\tau\beta)_{ij}$, $(\tau\gamma)_{ik}$, and $(\beta\gamma)_{jk}$ are the interactions between each pair of factors; $(\tau\beta\gamma)_{ijk}$ corresponds to the interaction among the three factors, and ε_{ijkl} is the error.[89]

S3.2. Combustion chamber (CV_2)

In the CV_2 a design of mixed levels 3×2^3 (Eq. (S17))[89] was considered in order to study the significance of the experimental factors on the energy efficiency of the combustion chamber (η_{CCG}, %). The factors under study and their respective levels are the biomass bulk density (560 kg/m^3 and 151 kg/m^3), the combustion-air/gasification-air ratio (2.8, 3.0, and 3.2), the combustion chamber design (combustion chamber 1 and 2), and the type of start (cold start and hot start). The values used for characterizing this control volume (combustion chamber) were gathered from the first experimental section for control volume 1.

S3.3. Gasification process in the cookstove (CV_3)

The control volume 3 was analyzed by a factorial experimental design 2^2, whose model is given by Eq. (S19)[89]. The factors and levels of the biomass bulk density (560 kg/m^3 and 151 kg/m^3) and the start type of gasification process (cold start and hot start) associated with the cookstove (CV_1) were assessed. The data of the gasification process are gathered during the first experimental section for control volume 1. The effects of the factors were studied on the following response variables: T_{max} (measured near the reactor wall, °C), fuel/air equivalence ratio (F_{rg}, dimensionless), biomass burning velocity (V_b, mm/min), biomass consumption rate ($\dot{m}_{bms}$, kg/h/m^2), dry base composition (%vol) and volumetric flow ($\dot{V}_{pg}$, Nm^3/h) and low heating value of the producer gas (LHV_{pg}, kJ/Nm^3), cold gas efficiency (CGE, %), producer gas yield (Y_{pg}, Nm^3_{pg}/kg_{bms}), and the biochar yield ($Y_{biochar}$, %).

$$Y_{ijk} = \mu + \tau_i + \beta_j + (\tau\beta)_{ij} + \varepsilon_{ijk} \quad \text{(S19)}$$

where μ is the global measure; τ_i is the effect of factor A; β_j is the effect of factor B; $(\tau\beta)_{ij}$ corresponds to the interaction between the two factors, and ε_{ijk} is the error.[89]

All the ANOVA analyses were performed using the Statgraphics Centurion XVI software, considering a confidence level of 95% (P value > 0.05). The effect of each factors and the effect of the interaction among factors on each response variable have been separately analyzed. Furthermore, in order to guarantee the validity of the results, the validation of the hypotheses of independence, normality, and constant variance in the residuals was done.[89]

S4. Fields of combustion air velocities through the combustion chamber

In Figure S1 and Figure S2, the air velocity fields for combustion chambers 1 and 2 are respectively presented, characterized through CFD simulations. The results are shown by rows due to the distribution of grooves in the combustion chamber. TR refers to the top row and LR corresponds to the lower row (see Figure 13).

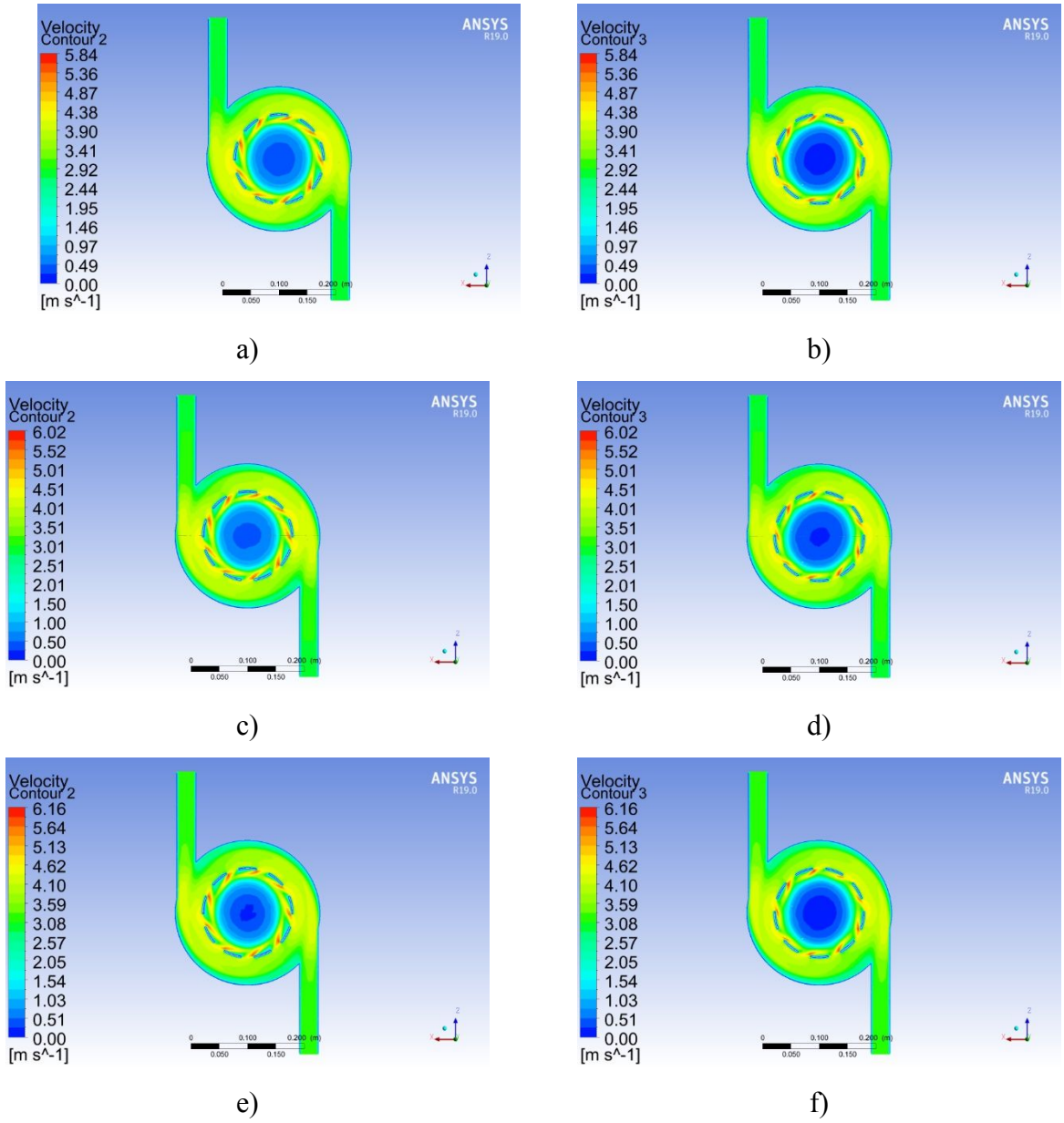

Figure S1. Combustion air velocity fields through the grooves of combustion chamber 1 (CCG1) for the different combustion-air/gasification-air ratios. a) CCG1-2.8-LR, b) CCG1-2.8-TR, c) CCG1-3.0-LR, d) CCG1-3.0-TR, e) CCG1-3.2-LR and f) CCG1-3.2-TR.

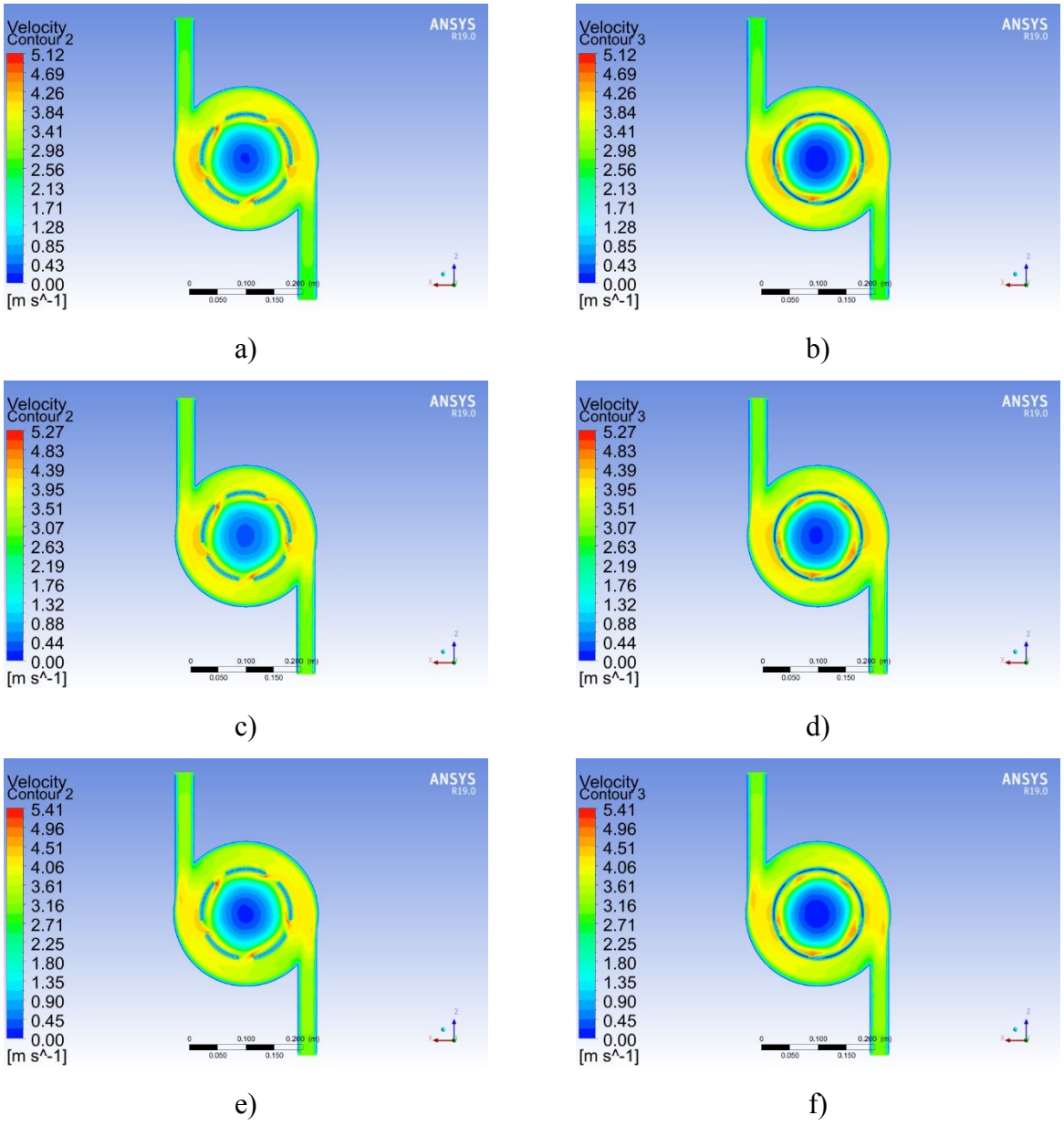

Figure S2. Combustion air velocity fields through the grooves of the combustion chamber 2 (CCG2) for the different combustion-air/gasification-air ratios. a) CCG2-2.8-LR, b) CCG2-2.8-TR, c) CCG2-3.0-LR, d) CCG2-3.0-TR, e) CCG2-3.2-LR and f) CCG2-3.2-TR.

S5. Specific energy consumption (kJ/L)

The specific energy consumption (Figure S3) was statistically affected by the biomass density and the combustion chamber design; meanwhile, the combustion-air/gasification-air ratio and the start type did not have a significant effect on this parameter (Figure S4). The average specific energy consumption for the pellets and chips was 1566.47 kJ/L (82.32 g/L) and 1678.72 kJ/L (99.63 g/L), respectively, resulting in a specific energy consumption ~7% higher for the chips compared to the pellets.[46] According to Eq. (S13), the higher specific energy consumption for the chips is attributed to a higher biomass consumption rate (~16%) compared to the pellets. As explained for the efficiency, the higher bulk density and higher packing factor of pellets favor the reduction of the biomass consumption rate. However, although the heating value of the biomass of the pellets was 13% higher concerning the chips, the biomass consumption rate reached with the chips was ~16% higher, generating an increase in the specific energy consumption for the chips. The specific energy consumption values found in this work are comparable and even lower to those reported for other improved cookstoves based on gasification, whose values ranged from 85 g/L to 140 g/L.[31,47,59]

Analyzing the combustion chambers design, for the cookstove fed with pellets under cold start - stage 1, the specific energy consumption was 1551.20 kJ/L for the combustion chamber 1 and 1662.43 kJ/L for the combustion chamber 2 (Figure S3). This corresponds to an energy consumption of 7% higher for the combustion chamber 2. In the case of hot start - stage 1 using the pellets, the TLUD cookstove reached values of 1443.82 kJ/L with the combustion chamber 1 and 1608.43 kJ/L with the combustion chamber 2, indicating an energy consumption ~10% higher for the combustion chamber 2. Furthermore, for the chips under cold start - stage 1, the specific energy consumption reached a value of 1483.84 kJ/L with the combustion chamber 1, and 1746.53 kJ/L for the combustion chamber 2 (specific energy consumption 15% higher for the combustion chamber 2). The cookstove fed with chips under hot start - stage 1 reached a specific energy consumption of 1605.80 kJ/L and 1678.72 kJ/L with the combustion chamber 1 and 2, respectively. This means an increase of 4% with the combustion chamber 2. The higher specific energy consumption found for the combustion chamber 2 with both biomass types (pellets and chips) is ascribed to a less effective mixing between the producer gas and the combustion air. This is due to a lower combustion air turbulence generated by the geometry and dimensions of the combustion chamber 2. This is explained in detail in the control volume 2 (Section 2.2). The less uniform mixing between the producer gas and the combustion air in the combustion chamber 2 leads to waste a high fraction of the released energy from the gas-gas combustion in the heating of the

combustion air. Therefore, the combustion temperatures decrease, generating a lower heat transfer to the cooking pot, and thus, the specific energy consumption increase.[53]

Even though the start type did not statistically affect the specific energy consumption, the specific energy consumption for the pellets was 1606.82 kJ/L under cold start - stage 1 and 1526.13 kJ/L in hot start - stage 1. This result in 5% decrease in the energy consumption during the hot start. Meanwhile, for the chips, the specific energy consumption reached 1615.18 kJ/L under cold start - stage 1 and 1742.26 kJ/L under hot start - stage 1 (specific energy consumption increased 7% under the hot start - stage 1). The contrary behavior that is observed between pellets and chips when going from cold start - stage 1 to hot start - stage 1 (specific energy consumption decreases for pellets and increases for the chips) is related to the cold gas efficiency (see analysis CV_3, Section 2.3). The higher heating value of the producer gas (~17%) of the pellets in the hot start - stage 1 with regard to the cold start - stage 1 favored the cold gas efficiency increment, which is ascribed to a higher producer gas power and a lower biomass energy supplied to the gasification process. While the chips showed a decrease in the cold gas efficiency of ~13% from the cold start - stage 1 to hot start - stage 1; the lower cold gas efficiency was due to an increase in the biomass consumption rate of ~22% from cold start - stage 1 to hot start - stage 1, which leads to increase the specific energy consumption under the hot start - stage 1.

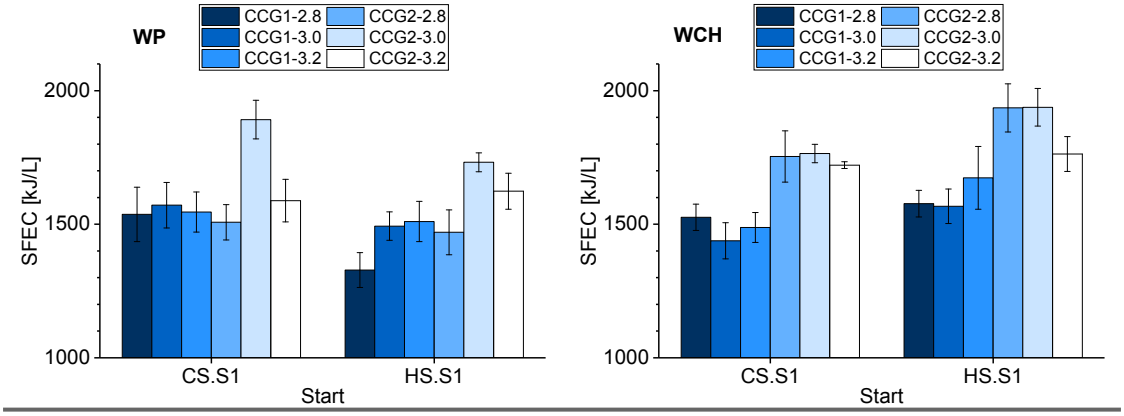

Figure S3. Specific energy consumption - SFEC (kJ/L) of the gasification-based cookstove in WBT-S1 under cold and hot starts (cold start - stage 1 (CS.S1) and hot start - stage 1 (HS.S1)).

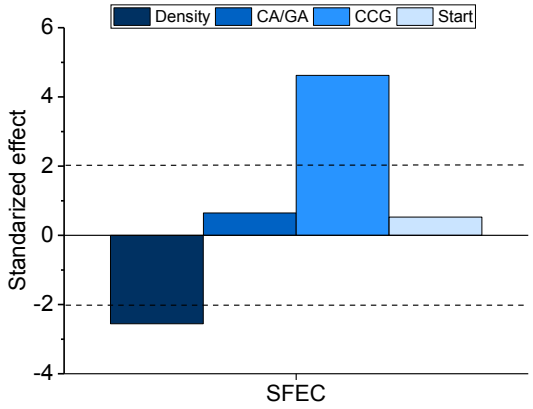

Figure S4. Pareto chart: effect of the biomass density, combustion-air/gasification-air (CA/GA) ratio, combustion chamber (CCG) design, and start type on the specific energy consumption - SFEC (kJ/L) of the gasification-based cookstove under cold start - stage 1 and hot start - stage 1.